200727031A

別紙１

厚生労働科学研究費補助金

エイズ対策研究事業

AZT誘発ミトコンドリア機能障害に対する分子治療方法の開発

平成１９年度　総括研究報告書

主任研究者　佐藤　岳哉

平成２０（２００８）年　４月

別紙２

研究報告書目次

目　　次

別紙３

厚生労働科学研究費補助金（エイズ対策研究事業）
（総括および分担）研究報告書

AZT誘発ミトコンドリア機能障害に対する分子治療方法の開発

主任研究者　佐藤　岳哉　東北大学大学院医学系研究科・助教

研究要旨

ヌクレオシド系抗HIV薬であるアジドチミジン(AZT)は、HIVに対する有効な作用を発揮する反面、重篤な心筋ミオパチーを誘発するが、その分子機構は不明な点が多い。今年度、私たちは、自ら見いだしたAZTを効率よくその活性化体に変換する酵素チミジル酸キナーゼ(tmpk)の変異型を用いて、活性化体の心筋に対する効果を検討するための実験系の作成に着手した。今年度は、実験系を作成することに成功した。次年度は、この実験系を用い、AZT誘発ミオパチーの分子機構について詳細に検討を行っていく。

分担研究者　柳澤　輝行
東北大学大学院医学系研究科・教授

A. 研究目的

抗HIV治療法として用いられているHAARTによる長期的副作用の内、AZTをはじめとするNRTIによるミトコンドリア機能障害による重篤な心筋ミオパチー等が、問題とされているが、その原因(分子機構)は未だ明らかとなっていない。本研究では、AZT代謝物が誘発するミトコンドリア機能障害の詳細な分子機構の詳細な解析から、ミトコンドリア機能障害を誘発する責任分子(群)すなわちAZT代謝物が標的とする分子(群)を同定することを目的とする。さらにこの副作用を持たない新規薬物、あるいは、副作用に対する保護作用を示す薬物をスクリーニングすることにより、HAART治療におけるAZT誘発ミトコンドリア機能不全症を防ぐ分子標的薬の開発を目指す。

B. 研究方法

1) 遺伝子導入用ベクター入手と組換え型tmpk調製

研究協力者のDr. Jeffrey A. Medin准教授(トロント大学・カナダ)より、チミジル酸キナーゼ(Tmpk)の野生型あるいは変異型cDNAを持つレンチウィルスベクターの分与を受け、これを使用した。

Tmpkに対する特異抗体を作製することを目的として、抗原として用いる組換え型tmpkの作製を行った。野生型tmpkのcDNAをインテイン蛋白質遺伝子の3'側に結合した融合遺伝子をもつプラスミドを構築し、大腸菌BL21(DE3)株に導入した。

2) AZTによる細胞死誘導の確認

1)で入手したレンチウィルスベクターを用いて、組み換えウィルスを作製し、マウス培養心筋細胞H9C2にこのウィルスを感染させることでtmpk遺伝子導入を行った。次に、非遺伝子導入細胞、tmpk野生型、変異型遺伝子導入細胞、tmpk遺伝子を持たないウィ

ルスベクターを感染させた細胞について、種々の濃度の AZT 存在下で培養後、MTT アッセイおよび細胞内 ATP 量の測定を行った。

（倫理面への配慮）

本研究において、倫理面において配慮が必要とされる研究は行わない。また、本研究においては、安全対策を必要とするレンチウィルスベクターの使用が含まれているが、申請者らはすでにこのウィルスベクター系を使うことに対する十分な安全対策を施した遺伝子組み換え実験計画を東北大学遺伝子組換え実験安全専門委員会に申請し、承認済みである。この試験計画を試行するにあたり、試験に使用した大腸菌、細胞および組換え DNA 分子は、オートクレーブ等により不活化して廃棄する。

C. 研究結果

1) 遺伝子導入用ベクター入手と組換え型 tmpk 調製

分与されたウィルスベクターの配列確認と大量調製を行った。野生型 tmpk の cDNA をインテイン蛋白質遺伝子の 3'側に結合した融合遺伝子をもつプラスミドを構築した。このプラスミドを大腸菌 BL21(DE3)株に導入し、得た形質転換体を 0.4 mM IPTG 存在下で 4 時間培養して、組換え蛋白質を得た。この蛋白質は細胞質内に可溶性の形で蓄積することが確認された。現在、組換え型 tmpk の大量調製を行っている。

2) AZT による細胞死誘導の確認

tmpk 変異型遺伝子を導入細胞においては、AZT の濃度依存的な細胞死誘導が観察されたが、対照群ではそれがみられなかった。また、tmpk 変異型遺伝子導入細胞は、10μM 以上の濃度の AZT 添加により、AZT 濃度依存性の顕著な細胞内 ATP 量の減少がみられた。一方、それ以外の細胞群では、100μM 以上の AZT 存在下において、有意な細胞内 ATP 量の低下が観察された。以上より、tmpk 変異型遺伝子導入細胞は、AZT 感受性が親株あるいは tmpk 野生型遺伝子導入細胞よりも亢進していることを確認した。

D. 考察

Tmpk 遺伝子搭載レンチウィルスを用いて、H9C2 細胞に遺伝子導入した細胞をモデル系として本研究に用いた。作製した細胞における導入遺伝子の発現確認は、特異抗体を用いる免疫学的検出で行う。この特異抗体を作製するための抗原として、組換え型 tmpk 作製を行った。この組換え蛋白質は、大腸菌の細胞質に可溶性で蓄積することを確認し、現在、組み換え蛋白質を大量調製している。この蛋白質を抗原として tmpk に対する特異抗体を作製し、この抗体を用いて、tmpk 遺伝子導入細胞における導入遺伝子の発現を確認する予定である。

Tmpk 遺伝子導入細胞を AZT 存在下で 4 日間培養し、その生存率、細胞内 ATP 量を測定したところ、tmpk 変異体遺伝子導入細胞において、生存率および ATP 量の顕著な低下がみられたのに対して、対照の細胞群ではそれがみられなかった。これは、tmpk 変異体蛋白質により、AZT が活性化体 AZT-TP へ変換され、ミトコンドリア機能障害を誘発したためと考えられる。これを証明するために、次年度の研究計画を遂行する必要がある。また、対照群の細胞においても、AZT 処理で細胞内 ATP 量の減少が見られたことは、AZT-MP もミトコンドリア機能に対して、何らかの影響を与えていることを示唆するものである。

次年度において、AZT 代謝物のミトコンド

リア機能障害に対する程度の比較、その分子機構などについて詳細に検討を行い、ミトコンドリア機能障害を誘発する責任分子(群)すなわちAZT代謝物が標的とする分子(群)を見いだし、さらにこの副作用を持たない新規薬物、あるいは、副作用に対する保護作用を示す薬物、すなわち、HAART治療におけるAZT誘発ミトコンドリア機能不全症を防ぐ分子標的薬の開発を行うこと目指す。

E. 結論

今年度、作製したtmpk遺伝子導入H9C2細胞は、AZT代謝物誘発ミトコンドリア機能障害の評価、およびその分子機構を検討することができるものであり、今後、これを用いて詳細な検討を行う必要がある。

F. 健康危険情報

特になし

G. 研究発表

1．論文発表

1) Takemoto J, Masumiya H, Nunoki K, **Sato T**, Nakagawa H, Ikeda Y, Arai Y, **Yanagisawa T**.
Potentiation of potassium currenta by β-adrenoceptor agonists in human urinary bladder smooth muscle cells: a possible electrical mechanism of relaxation.
Pharmacology 81, 251-258 (2008)

2) **Sato T**, Neschadim A, Konrad M, Fowler DH, Lavie A, Medin JA.
Engineered human tmpk/AZT as a novel enzyme/prodrug axis for suicide gene therapy. ***Mol Ther***. 15 (5), 962-970 (2007).

2．学会発表

海外

1) K. Maeda, M. Haraguchi, A. Kuramasu, **T. Sato**, K. Yanai, K. Fukunaga, **T. Yanagisawa**, J. Sukegawa.
Increase in Cell Surface Expression of Histamine H3 Receptor by a Chloride Intracellular Channel Protein.
47th Annual Meeting, The American Society for Cell Biology. December 1-5, 2007. Washington DC, USA.

2) **T. Sato**, J. Sukegawa, **T. Yanagisawa**.
Accumulation of an Active Metabolite of AZT, AZT-triphosphate, Induces Apoptosis of Jurkat Cells by Caspase-3 Activation.
47th Annual Meeting, The American Society for Cell Biology. December 1-5, 2007. Washington DC, USA.

国内

1) **佐藤岳哉**、佐藤友香、助川淳、**柳澤輝行**
抗腫瘍治療法としての新規自殺遺伝子治療法tmpk/AZTの応用（バイスタンダー効果の確認）
第58回日本薬理学会北部会　2007年9月27日、札幌

2) 前田恵、原口満也、倉増敦朗、**佐藤岳哉**、谷内一彦、福永浩司、**柳澤輝行**、助川淳
ヒスタミンH3受容体に結合する細胞内クロライドチャネルの機能解析
第58回日本薬理学会北部会　2007年9月27日、札幌

3) **Takeya Sato**, Jun Sukegawa, **Teruyuki Yanagisawa**
Molecular mechanisms of the induction of mitochondrial dysfunction by an active metabolite of AZT, AZT-triphosphate.
The 7th Japan-Korea Joint Symposium of Brain Sciences, and Cardiac and Smooth Muscles. 2007年12月8-12月10日、仙台

4) **柳澤輝行**、助川淳、**佐藤岳哉**
ヌクレオシド系抗ウィルス薬誘発性ミトコンドリア機能不全症の分子機構
第37回日本心脈管作動物質学会 2008年2月2日　仙台

5) **佐藤岳哉**、助川淳、佐藤友香、**柳澤輝行**
バイスタンダー効果発現における細胞接着装置の役割の関与について
第81回日本薬理学会年会
2008年3月17-19日　横浜

H. 知的所有権の出願・取得状況（予定を含む）

1. 特許取得
   なし。
2. 実用新案登録
   なし。
3.その他
   なし。

別紙４

研究成果の刊行に関する一覧表

書籍

著者氏名	論文タイトル名	書籍全体の編集者名	書　籍　名	出版社名	出版地	出版年	ページ
無し							

雑誌

発表者氏名	論文タイトル名	発表誌名	巻号	ページ	出版年
Takemoto J, Masumiya H, Nunoki K, **Sato T**, Nakagawa H, Ikeda Y, Arai Y, **Yanagisawa T.**	Potentiation of potassium currenta by β-adrenoceptor agonists in human urinary bladder smooth muscle cells: a possible electrical mechanism of relaxation.	*Pharmacology*	81	251-258	2008
Sato T, Neschadim A, Konrad M, Fowler DH, Lavie A, Medin JA.	Engineered human tmpk/AZT as a novel enzyme/prodrug axis for suicide gene therapy.	***Mol Ther.***	15 (5),	962-970	2007

Engineered Human tmpk/AZT As a Novel Enzyme/Prodrug Axis for Suicide Gene Therapy

Takeya Sato[1], Anton Neschadim[1,2], Manfred Konrad[3], Daniel H Fowler[4], Arnon Lavie[5] and Jeffrey A Medin[1,2,6]

[1]Division of Stem Cell and Developmental Biology, Ontario Cancer Institute, Toronto, Ontario, Canada; [2]Department of Medical Biophysics, University of Toronto, Toronto, Ontario, Canada; [3]Max Planck Institute for Biophysical Chemistry, Göttingen, Germany; [4]Center for Cancer Research, Experimental Transplantation and Immunology Branch, National Institutes of Health, Bethesda, Maryland, USA; [5]Department of Biochemistry and Molecular Genetics, University of Illinois at Chicago, Chicago, Illinois, USA; [6]Institute of Medical Sciences, University of Toronto, Toronto, Ontario, Canada

Gene therapy and stem cell transplantation safety could be enhanced by control over the fate of therapeutic cells. Suicide gene therapy uses enzymes that convert prodrugs to cytotoxic entities; however, heterologous moieties with poor kinetics are employed. We describe a novel enzyme/prodrug combination for selectively inducing apoptosis in lentiviral vector–transduced cells. Rationally designed variants of human thymidylate kinase (tmpk) that effectively phosphorylate 3′-azido-3′-deoxythymidine (AZT) were efficiently delivered. Transduced Jurkat cell lines were eliminated by AZT. We demonstrate that this schema targeted both dividing and non-dividing cells, with a novel killing mechanism involving apoptosis induction via disruption of the mitochondrial inner membrane potential and activation of caspase-3. Primary murine and human T cells were also transduced and responded to AZT. Furthermore, low-dose AZT administration to non-obese diabetic/severe combined immunodeficiency (NOD/SCID) mice injected with transduced K562 cells suppressed tumor growth. This novel suicide gene therapy approach can thus be integrated as a safety switch into therapeutic vectors.

Received 4 January 2007; accepted 16 January 2007; advance online publication 20 March 2007. doi:10.1038/mt.sj.6300122

INTRODUCTION

Leukemic transformation in gene therapy patients[1] has led to concern regarding the safety of integrating viral vectors. Nonetheless, these vectors offer efficient transduction and long-term gene expression. Research is directed toward increasing vector safety and reliability. A promising approach is to establish control over the fate of transduced cells. Incorporating an effective suicide gene can ensure that any malignant clones arising from insertion of the recombinant retroviral vector can be removed. Likewise, such control could be used for potential complications of embryonic stem cell transplantations, including therapy for malignant teratomas as developed in one recent study.[2]

The success of acyclovir against herpes simplex virus (HSV) infections[3] has engendered a strategy to kill tumors by delivering genes for drug-converting enzymes into malignant cells.[4] HSV thymidine kinase (HSV-tk) is involved in converting the prodrug ganciclovir (GCV) into its tri-phosphorylated form. GCV-triphosphate (TP) causes DNA chain termination during replication, ultimately leading to cell death.[5] In recent years, HSV-tk and mutants have become the most commonly employed enzymes for suicide gene therapy.[6,7] However, weaknesses of this strategy are the foreign origin of the transgene and the fact that overexpression of HSV-tk may simply redirect the rate-limiting step in the conversion to GCV-TP to the second enzyme in the pathway: guanylate kinase. Evidence is emerging, in particular from clinical trials,[8,9] that immune responses against HSV-tk limit the persistence of transduced cells. Successful suicide gene therapy, especially as a safety component for long-term correction of inherited diseases, for example, will thus require the expression of a non-immunogenic protein, either an overexpressed human enzyme or a minimally modified variant thereof.

The prodrug 3′-azido-3′-deoxythymidine (AZT) is converted through phosphorylation into AZT-triphosphate (AZT-TP).[10] AZT-TP inhibits replication of human immunodeficiency virus (HIV),[11,12] and to a lesser extent DNA replication in eukaryotic cells.[13] Safety profiles for this compound are well known. The rate-limiting step in the conversion of AZT to the toxic AZT-TP form is the phosphorylation of AZT-monophosphate (AZT-MP) to AZT-diphosphate (AZT-DP). This is catalyzed by cellular thymidylate kinase (tmpk), which has a low enzymatic efficiency for AZT-MP.[14] We predicted that increased AZT-TP concentrations, achieved by a strategy that accelerates the monophosphate-to-diphosphate conversion of the prodrug, would yield potent cytotoxicity. To improve the processing of AZT-MP to AZT-DP, we employed minimally modified tmpk mutants (F105Y and R16G-Large Lid (R16GLL)) with up to 200-fold enhanced activity for AZT-MP.[15,16] The F105Y variant encompasses a single substitution of the phenyalanine at position 105 to a tyrosine residue. The R16GLL variant was generated by exchanging 11 amino acid residues in the wild-type (WT) sequence with 13 residues from the *Escherichia coli* tmpk ortholog.

Correspondence: Jeffrey A. Medin, University Health Network, Room 406, 67 College Street, Toronto, Ontario, Canada M5G 2M1. E-mail: jmedin@uhnres.utoronto.ca

The safety aspect of suicide gene therapy relies on efficient delivery and stable expression of the cytotoxic effector. Lentiviral vectors (LVs) can transduce a wide range of dividing and non-dividing cell types with high efficiency, conferring stable, long-term transgene expression.[17,18] Reliable suicide gene therapy also requires that the overwhelming majority of transduced cells express the suicide gene. This can be ensured by introducing a cell-surface marker gene.[19] Transduced cells can be enriched based on expression of this marker. A cell-surface marker should be inert in itself, devoid of signaling capacity, and non-immunogenic.[20] Previously we have used a variety of cell-surface markers in this context: human CD24,[21] murine heat-stable antigen,[22] human CD25,[23] and a truncated form of LNGFR.[24]

Although human CD25 has been effective for our murine studies,[18,25] it is not useful for T-cell applications because endogenous expression is up-regulated in that population upon activation. Overexpression of a truncated form of LNGFR has promoted transformation of myeloid cells in an unusual, highly context-dependent manner.[26] Here, we adapt a novel truncated form of human CD19 (huCD19Δ) as our marker. CD19 is a 95-kd glycoprotein of the immunoglobulin superfamily that complexes with CD21, CD81, and Leu-13, which collectively function to modulate the activation threshold of the B-cell receptor.[27,28] As expression of CD19 and CD21 is restricted to B-cell lineages,[29] it is suitable for use in murine and human T cells. To further decrease signaling capacity, we have deleted the cytoplasmic tail[30] of CD19.

We have evaluated a novel prodrug/enzyme combination for suicide gene therapy. Catalytically improved variants of human tmpk along with huCD19Δ were efficiently delivered by novel bicistronic LVs, and selective clearance of cells *in vitro* and *in vivo* in response to increasing AZT concentrations was evaluated systematically. We present analysis of AZT sensitivity in transduced cells and further demonstrate a novel cytotoxic mechanism: that increased accumulation of intracellular AZT-TP decreases cell viability, partly owing to activation of a mitochondria-mediated apoptosis pathway. This system thus describes a practical choice for suicide gene therapy that can help to establish the next generation of safer integrating viral vectors. In addition, this schema can also be used to endow stem cells destined for utility in clinical transplantation with a reliable safety control system.

RESULTS

Synthesis of novel suicide LVs expressing modified tmpks and huCD19Δ

Figure 1 shows schematics of the recombinant LVs we constructed. Jurkat cells were transduced a single time (multiplicity of infection = 10). Five days later, huCD19Δ expression was examined. Although no huCD19Δ expression was observed on non-transduced (NT) Jurkat cells, more than 95% of transduced cells showed strong huCD19Δ expression (data not shown). Individual cell clones were isolated by limiting dilution and flow cytometry. The mean fluorescent intensity of huCD19Δ expressed on transduced cell clones showed similar values to each other (data not shown). Transduced cell clones were also examined by flow cytometry after intracellular immunostaining with rabbit anti-human tmpk. Basal expression of tmpk was detected in NT Jurkat cells. Cells transduced with LVs/tmpks showed increased tmpk expression, up to five times higher than in controls (data not shown). Western blots on cell lysates further demonstrated that expression levels of WT or variant forms of tmpk were similar in the transduced cell clones (data not shown).

Determination of intracellular AZT metabolites in LV/tmpk-transduced cells

To confirm functionality of the tmpk mutants, we measured the intracellular amounts of AZT metabolites using reverse-phase high-performance liquid chromatography (HPLC). Cells expressing the R16GLL mutant tmpk efficiently converted AZT-MP into AZT-DP and then, by other kinases, into AZT-TP, whereas the main metabolite that accumulated in the NT-Jurkat cells was AZT-MP (**Figure 2**). Interestingly, we observed no significant increases in the accumulation of AZT-TP or induction of cell death (see below) in the cells overexpressing WT tmpk itself (data not shown). This demonstrates the importance of using engineered enzymes optimized for AZT-MP phosphorylation. The ratio of AZT-TP to AZT-MP in each cell population was calculated from the values of the area under the curve of each chromatogram. **Figure 2** shows that overexpression of the R16GLL and F105Y mutants induced a pronounced increase in the AZT-TP/AZT-MP ratio compared with controls. Mitochondrial fractions were enriched from control LV-internal ribosome entry site (IRES) huCD19Δ and test LV-R16GLLtmpk-IRES-huCD19Δ-transduced cell clones and analyzed using HPLC for levels of AZT metabolites. In the control cells, AZT-MP, AZT-DP, and AZT-TP were observed at appreciable levels. In contrast, only AZT-DP and AZT-TP were observed in the mitochondria of the cells expressing the R16GLL tmpk mutant (data not shown).

AZT sensitivity of LV/tmpk-transduced cells

By itself, transduction of Jurkat cells with LVs engineering expression of controls or our modified suicide genes and huCD19Δ did not affect proliferation (data not shown). To examine the effect of exposure to AZT on cell viability, we incubated the tmpk-expressing cells with increasing concentrations of AZT and after 4 days determined the percentage of living cells (**Figure 3**). Transduced cells expressing the AZT-MP catalytically-optimized tmpk mutants F105Y or R16GLL were minimally viable upon addition of AZT in a dose-dependent manner ($P < 0.0001$). In contrast, limited cell killing, even at high doses of AZT up to 1 mM, was observed in the control cells.

As we observed the formation of nuclear apoptotic bodies by 4′-6-diamidino-2-phenylindole staining in the tmpk mutant–expressing cells treated with prodrug (data not shown), we speculated that active metabolites of AZT induced cell death by apoptosis. To confirm this, we stained the AZT-treated tmpk-expressing cells with Annexin V and performed flow cytometric analyses. In response to 100 μM AZT exposure, early apoptotic indices of cells expressing the F105Y and the R16GLL tmpk mutants were significantly increased ($P < 0.0001$) compared with those in the absence of AZT treatment (9.5 ± 0.8–fold and 8.3 ± 0.4–fold increases, respectively).

HSV-tk-mediated cell killing requires cellular proliferation for the cytotoxic effect, through DNA chain termination mediated by the anti-metabolites produced.[31] We evaluated whether the

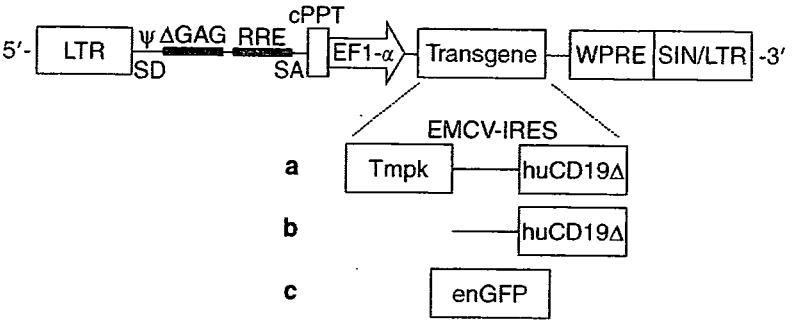

Figure 1 Schematic diagram of recombinant lentiviral vector (LV) constructs used in these studies. (**a**) LV-thymidylate kinase-IRES-huCD19Δ, (**b**) LV-IRES-huCD19Δ, (**c**) LV-enhanced green fluorescent protein. cPPT, central polypurine tract; EF-1α, elongation factor 1α promoter; LTR, long terminal repeat; RRE, Rev responsive element; SA, 3′ splice acceptor site; SD, 5′ splice donor site; SIN, self-inactivating LTR; WPRE, woodchuck hepatitis virus post-transcriptional regulatory element; ψ, human immunodeficiency virus packaging signal.

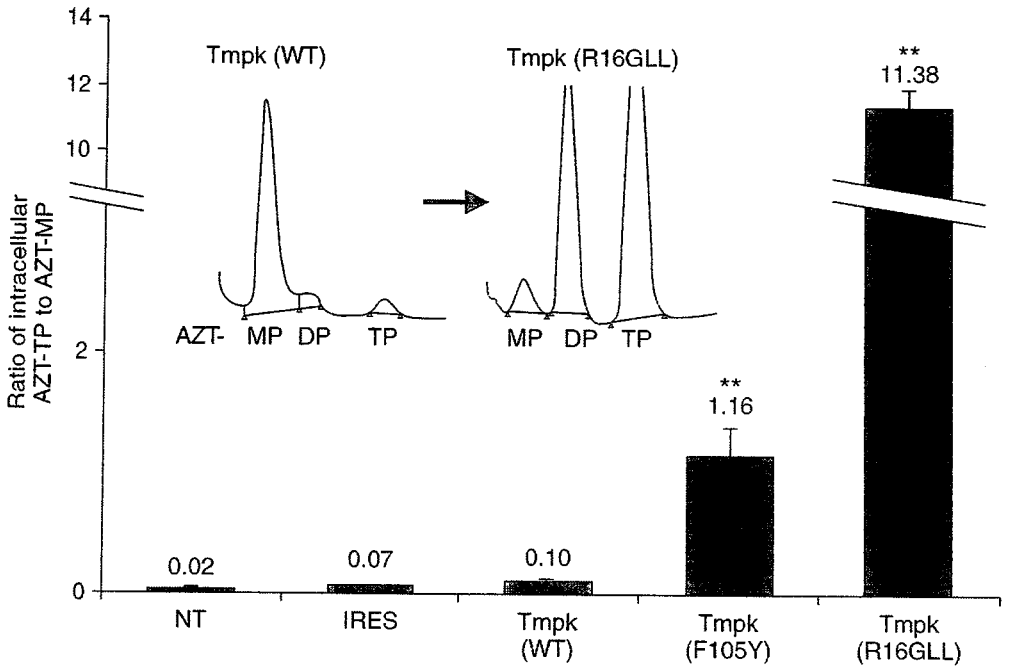

Figure 2 Determination of 3′-azido-3′-deoxythymidine (AZT) metabolites in transduced clonal Jurkat cell lines and controls treated for 36 hours with 100 μM AZT. Inset: representative chromatograms for the non-transduced cells and the thymidylate kinase R16GLL mutant–expressing cells. Peaks corresponding to AZT-monophosphate, AZT-diphosphate, and AZT-triphosphate are labeled. Bar graph: comparison of the ratio of the intracellular AZT-TP to AZT-MP in the AZT-treated cells. Data are mean ± standard error of the mean ($n = 3$). The statistical differences were evaluated by one-way analysis of variance followed by a Bonferroni post hoc test with the level of significance set at $P < 0.05$. $^{**}P < 0.01$ versus wild-type transduced cells.

cytotoxic events of AZT on tmpk-expressing cells were also dependent on cellular proliferation. We cultured transduced cells with or without 100 μM AZT in the presence of indirubin-3′-monoxime to arrest cell cycle progression. After incubation for 4 days with 5 μM indirubin-3′-monoxime, cells were arrested at the G_2/M-phase (data not shown). By treating the cells with 100 μM AZT in the presence of 5 μM indirubin-3′-monoxime, the apoptotic indices of the F105Y- and R16GLL-expressing cells were still significantly increased (2.3 ± 0.4-fold and 2.2 ± 0.2-fold, respectively) compared with the indices of cells without AZT treatment ($P = 0.0011$). No significant increases were seen in the apoptotic indices of control cells (data not shown). This suggests that the induction of apoptosis by AZT in the tmpk mutant–expressing cells is, in part, independent of their proliferation status.

Transduction and AZT sensitivity of primary human and mouse T cells

Next, primary human and mouse T cells were transduced once with the LV-tmpk constructs (multiplicity of infection = 20). We did not use the R16GLL mutant as this version contains a bacterial tmpk sequence, which could eventually be immunogenic *in vivo*. In contrast, the F105Y variant contains a single amino acid change at position 105. After 6 days of culture, transduced T cells were assessed for huCD19Δ expression. Although nominal NT cells expressed huCD19Δ, more than 50% of LV-transduced primary murine T cells stably expressed the marker (data not shown). In the same way, more than 60% of transduced human T cells stably expressed huCD19Δ (data not shown). These percentages are considerable given that expression of downstream genes in

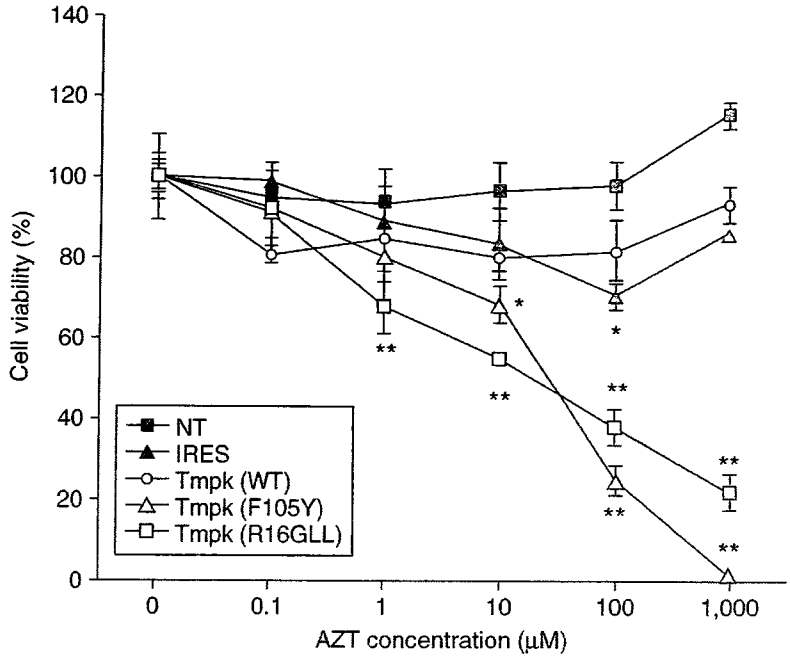

Figure 3 Measurement of 3′-azido-3′-deoxythymidine (AZT) sensitivity of clonally-derived Jurkat cells transduced with thymidylate kinase-IRES-huCD19Δ and control lentiviral vectors. Cell viability was measured by proliferation assay following 4 days incubation with or without AZT. The results were determined as a percentage of the A595 nm value from the assay. The negative control values (without AZT) and the values without cells were deemed to be 100 and 0%, respectively. Data are presented as mean ± standard error of the mean (n = 3). The statistical significance of experimental observation was determined by one-way analysis of variance followed by a Dunnett post hoc test with the level of significance set at $P < 0.05$ compared with the values of the control group of cells that were not treated with AZT. $^*P < 0.05$ and $^{**}P < 0.01$ versus cells without AZT treatment in each group.

bi-cistronic cassettes may be less than 10% that of upstream genes.[32] To test AZT sensitivity, transduced human T cells were exposed to 100 μM AZT for 4 days and induction of apoptosis was measured by Annexin V staining. Although the early apoptotic indices of primary NT human T cells were somewhat increased by AZT exposure at this dose, the apoptotic index of cells expressing the F105Y tmpk mutant was significantly increased ($P < 0.0001$) compared to the index of cells without AZT treatment (4.0 ± 0.3-fold; data not shown).

Novel suicide mechanism utilized by the tmpk/AZT axis

AZT inhibits HIV replication. Yet HIV-AIDS patients treated with AZT sometimes develop toxic mitochondrial myopathy through induction of mitochondrial biochemical dysfunction.[33–35] We sought to determine whether cellular apoptosis induction in our study involved this mechanism. We measured the mitochondrial inner membrane potential in intact LV-tmpk mutant–transduced cells following AZT treatment. Here we applied a fluorescent probe, 5,5′,6,6′-tetrachloro-1,1′,3,3′-tetraethylbenzimidazolylcarbocyanine iodide (JC-1), and examined living cells by flow cytometry. The dye JC-1 emits a green fluorescence at low mitochondrial membrane potential.[36] At higher membrane potentials, JC-1 forms red fluorescence-emitting "J-aggregates." We found that a significant increase ($P < 0.0001$) in the loss of mitochondrial inner membrane potential occurred in both the F105Y- and the R16GLL-expressing Jurkat cells (**Figure 4a**) after 4 days of AZT treatment compared with controls. This effect was clearly present in the variant tmpk-expressing Jurkat cells but not in the WT-overexpressing cells from day 1. Indeed, control groups treated with AZT did not demonstrate a similar loss of membrane potential at any point (**Figure 4a**).

Caspase-3 is a key molecule in the cellular apoptosis pathway; loss of mitochondrial inner membrane potential induces caspase-3 activation.[37] We next evaluated caspase-3 activation in transduced cells treated with AZT. F105Y- or R16GLL-expressing cells treated with AZT showed a significant increase in the percentage of activated caspase-3-positive cells compared with untreated or control cells (**Figure 4b**). Interestingly, tmpk WT–overexpressing cells treated with AZT showed a slight, but significant, increase in the percentage of active caspase-3-positive cells. Taken together, our data demonstrate that apoptosis induction by prodrug in the tmpk mutant–expressing cells is due to the activation of caspase-3 resulting from the increase in the loss of the mitochondrial membrane potential caused by the accumulation of AZT-TP.

In vivo killing of LV/tmpk-transduced cells mediated by AZT

We next examined killing of the LV/tmpk mutant–transduced cells in an *in vivo* tumor model. K562 erythroid leukemia cells were transduced with our recombinant LVs. Since transduction with the F105Y LV was modest (~68% huCD19Δ-positive cells; data not shown), these cells were enriched by fluorescence-activated cell sorting (FACS) using anti-human CD19 conjugated to phycoerythrin. Afterward, more than 95% of cells were huCD19Δ-positive (data not shown), confirming the auxiliary utility of this marker for immuno-affinity enrichment. Minimal differences in growth characteristics of the transduced cells

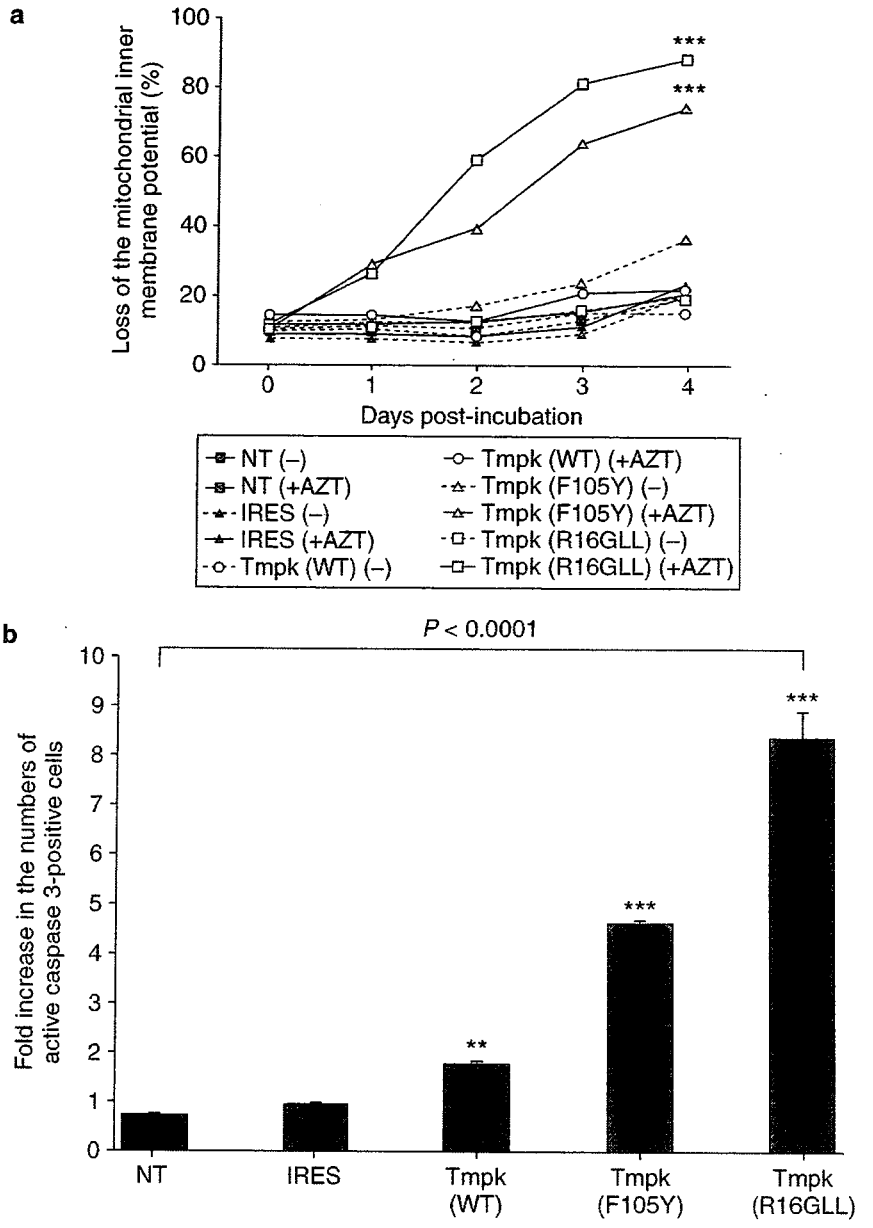

Figure 4 Analysis of the mechanism of induction of apoptosis by 3′-azido-3′-deoxythymidine (AZT) in the thymidylate kinase (tmpk) mutant–expressing cells. (**a**) The tmpk mutant–expressing cells treated with AZT showed an increase in the loss of mitochondrial membrane potential. Following 4 days incubation with or without 100 μM AZT, cells were stained with 5,5′,6,6′-tetrachloro-1,1′,3,3′-tetraethylbenzimidazolylcarbocyanine iodide for 15 minutes at 37 °C and were then analyzed by flow cytometry. To determine the effect of AZT on the increase in the loss of mitochondrial membrane potential at Day 4, the statistical differences were evaluated by one-way analysis of variance (ANOVA) followed by a Bonferroni post hoc test with the level of significance set at $P < 0.05$. ***$P < 0.001$ ($n = 3$). (**b**) Activation of caspase-3 in transduced cells by AZT treatment. Cells were cultured for 4 days with or without 100 μM AZT. To compare the effect of AZT on activation of caspase-3 in each group, measurements of flow cytometry obtained from the cells treated with AZT were normalized by dividing by the values for cells without AZT. Data are mean ± standard error of the mean ($n = 3$). The statistical differences were evaluated by one-way ANOVA followed by a Bonferroni post hoc test with the level of significance set at $P < 0.05$. **$P < 0.01$ and ***$P < 0.001$ versus non-transduced cells.

were observed (data not shown). Next, 2×10^7 transduced K562 cells were injected into non-obese diabetic/severe combined immunodeficiency (NOD/SCID) mice. Starting 1 day after the cell injection, the mice received daily injections of AZT (2.5 mg/kg/day) or vehicle for 2 weeks. Mice were killed when tumors reached approximately 1.5 cm^3; in animals injected with NT K562 cells, this endpoint occurred within 2 weeks. Mice not receiving AZT treatment quickly developed large tumors in a time-dependent manner (**Figure 5**). In contrast, the growth of K562 cells transduced with either of the tmpk mutant LVs (F105Y or R16GLL) was strongly inhibited by daily AZT injection, and the effects were sustained over time (**Figure 5**). This result, using this low dose of 2.5 mg/kg/day of AZT, is even more striking given safety data for mice treated with AZT at 270 mg/kg/day for 15 days, which showed only marginal hematoxicity and no nephrotoxicity.[38] This is also well below the Food and Drug Administration recommended dose of 1,200 mg/day acutely (17.1 mg/kg/day for a 70 kg individual) and 500–600 mg/day

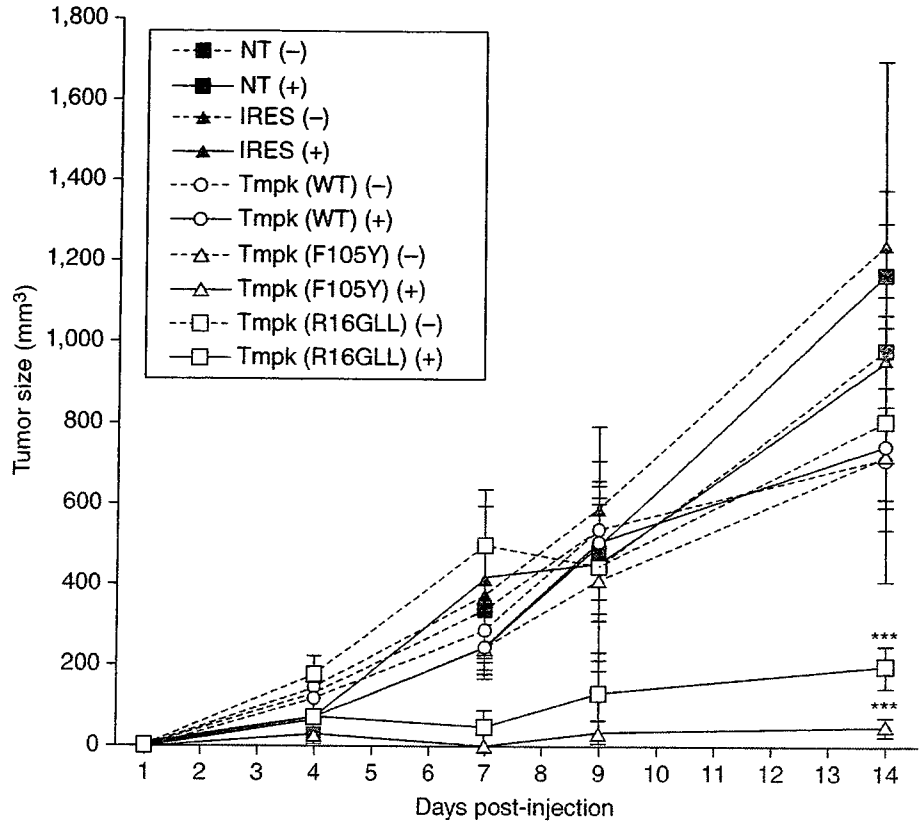

Figure 5 Daily injection of 3′-azido-3′-deoxythymidine (AZT) prevents growth of K562 cells transduced with lentiviral vector (LV)-thymidylate kinase mutant in non-obese diabetic/severe combined immunodeficiency (NOD/SCID) mice. NOD/SCID mice were subcutaneously injected into the dorsal right flank with 2×10^7 of either the non-transduced (NT) or the LV-transduced K562 cells. Starting 1 day after the cell injection, the mice received daily intraperitoneal injections of AZT (2.5 mg/kg/day) for 2 weeks and tumor volume was monitored. Data are mean ± standard error of the mean ($n = 5$ for each group). Statistical differences in tumor sizes at Day 14 were evaluated by one-way analysis of variance followed by a Bonferroni post hoc test with the level of significance set at $P < 0.05$. ***$P < 0.001$ versus NT without AZT injection.

(7.1–8.6 mg/kg/day for a 70 kg individual) for long-term treatment of HIV infection in humans.

DISCUSSION

Suicide gene therapy has a number of manifestations: direct tumor reduction, clearance of transplanted cells, and as a future safety component in clinical protocols involving integrating viral vectors. Such a portable safety system could also have benefits in stem cell transplantation.[2] Yet, to date, suicide gene therapy has not been fully effective. Here we have shown that overexpression of rationally designed mutant forms of human tmpk with improved kinetics significantly reduces cellular viability following AZT treatment both *in vitro* and *in vivo*. Thus, an otherwise minimally cytotoxic prodrug can be made highly cytotoxic by virtue of accelerating its activation. Overexpression of the WT enzyme alone was not sufficient; engineered enzymes with improved kinetics are required. Our results also demonstrate that the mechanism of AZT-induced apoptosis is associated with loss of mitochondrial inner membrane potential and activation of caspase-3 in the tmpk mutant–expressing cells. This mechanism differs from most previous suicide schemas and is likely beneficial, as it allows killing of non-dividing cells.

Tmpk catalyzes the rate-limiting second phosphorylation step in the activation of AZT.[14] AZT was the first effective treatment for AIDS patients;[11,12] however, long-term use can induce a severe myopathy characterized by alterations in mitochondria as a result of accumulation of AZT-MP.[34,39,40] Inhibition of the mitochondrial inner membrane potential has also been found in long-term AZT-treated rats.[35] We observed that accumulation of AZT-TP in the tmpk mutant–expressing cells abolished the inner membrane potential of mitochondria (**Figure 4a**) and increased the apoptotic index as a result of the activation of caspase-3 (**Figure 4b**). Yet the mechanism of this inhibition remains to be addressed in detail.

The use of huCD19Δ as a cell-surface marker facilitated an increase in the ratio of gene-modified cells by immuno-affinity enrichment. The contribution of the CD19 cytoplasmic domain to signal transduction has been previously assessed *in vitro* by transfecting the cells with a truncated form,[41] and *in vivo* using mice that express truncated human CD19.[30] These studies demonstrated that the cytoplasmic domain of CD19 is crucial for signaling and for the *in vivo* function of the CD19/CD21/CD81/Leu-13 complex. This indicates that the huCD19Δ form that we have employed is unlikely to signal. However, the effect of expression of huCD19Δ in target cells of interest warrants further examination. Of note, we have recently shown that use of a co-expressed surface antigen from bi-cistronic LVs allows clearance of transduced cells by other methods such as specific toxin-conjugated antibodies, thereby providing a further safety mechanism (J.A.M, manuscript submitted).

We have demonstrated that safety issues for integrating gene transfer can be alleviated using recombinant LVs that lead to expression of rationally engineered activating enzymes. Furthermore, NOD/SCID mice xenografted with transduced K562 cells (either F105Y or RG16LL expressing) and treated with AZT showed substantive suppression of tumor growth *in vivo* (**Figure 5**). Indeed, the transduced cancer cells are effectively eliminated at low systemic concentrations of AZT. This strategy can prevent cancer-related complications of gene therapy, as our killing schema involving the mitochondrial death pathway is robust enough that even immortalized cancer cells die by this mechanism. This could also lead to novel strategies in cancer treatment to overcome drug resistance that stems from mutations in cellular enzymes adversely affecting prodrug activation.

Adoptive immunotherapy using T cells is an effective approach to treat hematological malignancies.[9,42–45] Graft-versus-host disease, however, remains a major problem following non-T-cell-depleted allogeneic bone marrow transplantation.[46] An efficient *in vivo* safety switch for elimination of gene-modified T cells in the event of graft-versus-host disease would be useful. GCV has been used to deplete HSV-tk-expressing allogeneic lymphocytes following bone marrow transplantation.[42,43] Depletion is not always complete, however, and host immune responses against cells expressing this foreign enzyme can impair their function and persistence.[8,9] In addition, T-cell responses are to multiple epitopes, suggesting that modification of immunogenic sequences in HSV-tk would be ineffective in ablating this full response.[9] The use of human proteins as alternative suicide effectors is less likely to induce an immune response. Furthermore, most bone marrow transplantation patients are on prophylactic GCV to minimize cytomegalovirus infections, which decreases the clinical utility of HSV-tk-based suicide gene therapy. One of our current efforts seeks to utilize the novel LV-tmpk approach we have developed for reduction of graft-versus-host disease. Indeed, to confirm the utility of catalytically improved variants of human tmpk as an *in vivo* safety switch, we have already transduced primary cultured human and murine T cells in high transduction efficiencies and demonstrated specific killing upon addition of AZT (see above).

In conclusion, suicide gene therapy using LV-mediated human tmpk gene delivery combined with AZT as an effective prodrug has potential to be a potent safety element in controlling the fate of gene-modified cells.

MATERIALS AND METHODS

cDNA cloning of human CD19 and construction of LV shuttle vector. Total RNA was extracted from the human Burkitt's lymphoma cell line (Raji) using the TRIZOL reagent (Invitrogen, Carlsbad, CA). cDNA templates were generated from total RNA by reverse transcription using oligo-dT primer and Superscript II reverse transcriptase (Invitrogen). The cDNA of full-length huCD19 was obtained by PCR using platinum Hifi *Taq* DNA polymerase (Invitrogen) and primers CD19 F1 and CD19 R1 (described below). The amplified PCR product was directly ligated into the TA vector, pPCR-script SK (+) (Stratagene, La Jolla, CA), to give pPCR-huCD19full. A truncated form of huCD19 (huCD19Δ) that has the extracellular and transmembrane domains but lacks the cytoplasmic domain was generated by inverse PCR from pPCR-huCD19full using primers CD19 F2 and CD19 R2 (described below) to give pPCR-huCD19Δ. The F2 primer has a complementary sequence to the stop codon just after the end of the transmembrane domain. Following sequence confirmation of the cDNA inserts in pPCR-huCD19Δ, the cDNA fragments were then isolated and subcloned into the *Eco*RI site of the shuttle vector pSV-IRES, which has a sequence for an IRES element from the encephalo-myocarditis virus, to give pSV-IRES-huCD19Δ. The primer sequences used for subcloning of the human CD19 cDNA were as follows: CD19 F1: 5′-atgccacctcctcgcctcctcttcttcc-3′ and CD19 R1: 5′-tcacctggtgctccaggtgccc-3′. The truncated CD19 construct was made by inverse PCR using the following primers: CD19 F2: 5′-ccgccaccgcg gtggagctccag-3′ and CD19 R2: 5′-ttaaagatgaagaatgcccacaaggg-3′.

Subcloning of human tmpk cDNA and construction of bi-cistronic LVs. To subclone the cDNA for WT human tmpk, peripheral blood mononuclear cells were isolated from heparinized blood obtained from healthy donors by Ficoll-Hypaque density gradient separations (GE Healthcare Biosciences, Inc., Freiburg, Germany). The WT human tmpk cDNA was amplified by PCR using first-strand cDNA generated from peripheral blood mononuclear cell RNA by the method above. PCR products containing the WT tmpk cDNA were subcloned into pPCR-scriptSK (+) and sequenced. Mutant forms of tmpk, denoted F105Y and R16GLL, had been generated previously.[15,16] The cDNAs for the WT and each mutant form of tmpk were first subcloned into a shuttle vector (pSV-IRES-huCD19Δ) to construct bi-cistronic expression cassettes that allow simultaneous expression of a single mRNA strand encoding the suicide gene and huCD19Δ. Each of the constructs was then subcloned downstream of the internal EF1α promoter into an HIV-1-based recombinant LV plasmid, pHR′-cPPT-EF-W-SIN.[18] As a control for the transduction experiments, we constructed a pHR′-cPPT-EF-IRES-huCD19Δ-W-SIN LV by subcloning the IRES-huCD19Δ cassette from the pSV-IRES-huCD19Δ plasmid into pHR′-cPPT-EF-W-SIN. In addition, we used the pHR′-cPPT-EF-enGFP-W-SIN LV[24] containing the enhanced GFP cDNA.

Preparation of high-titer LV. Vesicular stomatitis virus glycoprotein–pseudotyped LVs, including an enhanced GFP-marking vector, were generated by transient transfection of 293T cells with a three-plasmid system (the aforementioned pHR′ plasmid constructs, the packaging plasmid pCMVΔR8.91, and the vesicular stomatitis virus glycoprotein envelope encoding plasmid pMD.G) using $CaPO_4$ precipitation.[17] Viral supernatants were harvested 48 hours later, passed through a 0.45-μm filter, and suspended in phosphate-buffered saline containing 0.1% (w/v) bovine serum albumin after ultracentrifugation at 50,000*g* for 2 hours at 4 °C. The concentrated viral supernatants were serially diluted and titered on 293T cells. Transgene expression in transduced cells was assessed 72 hours later using a FACS Calibur (BD Biosciences, San Jose, CA) after staining of the transduced and control cells with monoclonal mouse anti-human CD19 conjugated with phycoerythrin (BD Biosciences, San Jose, CA) or for enhanced GFP expression. Analysis of the data was performed using Cell Quest software (BD Biosciences). Titers of each of the concentrated LVs used were more than 10^8 productively infectious particles/mL as measured by functional enhanced GFP and huCD19Δ expression (data not shown).

Transduction and analysis of transgene expression by western blot and flow cytometric analyses. Cells of the human T lymphoma cell line, Jurkat, and of the human erythro-leukemic cell line, K562, were maintained in Roswell Park Memorial Institute 1640 medium supplemented with 10% fetal bovine serum (CPAA Laboratories, Etobicoke, ON), 100 U/ml penicillin, and streptomycin to 100 μg/ml (both Sigma, Oakville, ON). Cells were infected with concentrated virus stocks using a multiplicity of infection of 10 in the presence of 8 μg/ml protamine sulfate. Infected cells were then kept in culture for 5 days before evaluating gene transfer efficiency. Gene transfer efficiencies were measured by

flow cytometry as described above. Individual clone cell lines were used for all subsequent experiments. They were derived by limiting dilution and selected based on comparable huCD19Δ expression as determined by flow cytometry (above).

To compare the relative expression levels of tmpk by flow cytometry, the transduced cells were first fixed with 4% buffered formalin for 15 minutes and then permeabilized by treatment with phosphate-buffered saline containing 0.1% Triton X-100 for 10 minutes. Cells were incubated with 20% normal goat serum for 30 minutes and then incubated with rabbit anti-human tmpk (diluted 1:500) for 1 hour. The cells were further incubated with goat anti-rabbit IgG conjugated to Alexa488 (diluted 1:500, Molecular Probes Inc., Eugene, OR) for 1 hour. All incubations were performed at room temperature. For western blots, total cell lysates were resolved by 12% sodium dodecyl sulfate polyacrylamide gel electrophoresis and transferred onto polyvinylidene difluoride filters (Millipore, Billerica, MA). Filters were blocked with 5% fat-free skim milk in tris-buffered saline with 0.05% Tween-20. Human tmpk overexpression was elucidated using rabbit anti-human tmpk (diluted 1:5,000). Lysate protein loading amounts in each lane were confirmed with a murine anti-β-actin antibody (Chemicon, Temeula, CA) diluted 1:5,000. Blots were probed with appropriate horseradish peroxidase–conjugated secondary antibodies and proteins were detected using an enhanced chemiluminescence kit (Perkin Elmer, Norwalk, CT) and Kodak BioMAX XAR film.

HPLC for AZT metabolites. Cells were cultured in the presence of 100 μM AZT for 36 hours. A total of 10^7 cells were homogenized by sonication in 100 μl of 5% (w/v) trichloroacetic acid. The supernatant was collected after centrifugation at 10,000 *g* for 15 minutes at 4 °C. Trichloroacetic acid was removed by extraction with an equal volume of 20% *tri*-n-octylamine in pentane. The neutralized aqueous fraction was directly injected into the HPLC machine (Waters, Milford, MA). Separation of AZT and its metabolites was performed on a C18 column (Waters), with a mobile phase composed of 0.2 M phosphate buffer containing 4 mM tetrabutylammonium hydrogen sulfate (pH 7.5) and acetonitrile in the ratio of 97:3 (v/v)[47] at a flow rate of 1.5 ml/min. The UV absorbance was monitored at 270 nm. Standards for each AZT metabolite (AZT-MP, AZT-DP, and AZT-TP) were purchased from Moravek Biochemicals (Brea, CA). Five million cell equivalents were injected and analyzed in triplicate. Mitochondria-enriched fractions from 10^9 cells of LV-IRES-huCD19Δ- and LV-R16GLLtmpk-IRES-huCD19Δ-transduced clones treated with 100 μM AZT were prepared using a method described elsewhere (AT Ho and E Zacksenhaus, manuscript submitted). Specifically, cells were lysed mechanically in a glass grinder in 5 ml of ice-cold S100 buffer (20 mM HEPES-KOH (pH 7.5), 10 mM KCl, 1.5 mM $MgCl_2$, 1 mM Na·EDTA, 1 mM Na·EGTA, 1 mM DTT, and 0.1 mM PMSF). Lysate was then centrifuged at 700 *g* for 20 minutes at 4 °C; supernatant was collected and centrifuged further at 10,000 *g* for 30 minutes at 4 °C. Next the supernatant was collected as the cytosol fraction, and the mitochondria-enriched pellet was washed with 1 volume of ice-cold S100 buffer, followed by centrifugation at 10,000 *g* for 30 minutes at 4 °C. AZT metabolites were extracted from the pellet as before and injected into the HPLC in duplicate.

Determination of AZT sensitivity of tmpk-transduced Jurkat cells. Transduced Jurkat cells and single-cell clones were seeded in 96-well plates (2×10^5 cells/well) in 200 μl of the Roswell Park Memorial Institute medium described above, with increasing concentrations of AZT (0, 0.1, 1, 10,100 μM, and 1 mM). The medium was changed daily. After 4 days of culture, cell viability was determined using the Cell Titer 96 Aqueous One Solution Cell Proliferation Assay kit (Promega, Madison, WI).

For evaluation of the induction of apoptosis, treated Jurkat clonal cells were stained with Annexin V. In brief, cells were seeded in a 24-well plate (10^6 cells/well) in 1 ml medium with or without 100 μM AZT. After 4 days of culture, Annexin V staining was performed according to the manufacturer's protocol (Annexin V-APC; BD Pharmingen, San Diego, CA). To test whether AZT-mediated cell killing depends on the cellular proliferation, indirubin-3′-monoxime (final concentration 5 μM; Sigma-Aldrich, St. Louis, MO) was added simultaneously with 100 μM AZT to the culture. To simplify comparative studies, a relative apoptotic index was calculated. Here data obtained were normalized by dividing results from AZT-treated cells in each condition by the results obtained without added AZT. Values were reported as fold increases. Statistical significance between groups was calculated by analysis of variance.

Transduction of primary T cells with LVs and evaluation of induction of apoptosis after AZT exposure. Human T lymphocytes were isolated from peripheral blood mononuclear cells contained within heparinized blood obtained from healthy human donors by Ficoll-Hypaque separations. Mouse T cells were prepared from B-cell-depleted splenocyte preparations using goat anti-mouse IgG beads (BioMag, Qiagen, Mississauga, ON). T cells were activated using anti-CD3- and anti-CD28-coated beads[48] in a ratio of 1:3 (cells to beads) with 20 IU/ml recombinant human interleukin-2 (R&D Systems, Minneapolis, MN) for 3 days. Cells were infected with concentrated virus stocks for 3 hours on ice using an indicated multiplicity of infection in the presence of 8 μg/ml protamine sulfate. Infected cells were then kept in culture for 5 days before gene transfer efficiency was evaluated. Gene transfer efficiencies were measured by flow cytometry using a monoclonal anti-human CD19 antibody conjugated with phycoerythrin as described above. Induction of apoptosis following AZT exposure was evaluated by Annexin V staining as above.

Measurement of mitochondrial inner membrane potential and activation of caspase-3. Transduced cells (10^6) were treated with 100 μM AZT for 4 days or left untreated. To detect changes in the mitochondrial inner membrane potential, the cells were incubated with 5,5′,6,6′-tetrachloro-1,1′,3,3′-tetraethylbenzimidazolylcarbocyanine iodide (JC-1, Molecular Probes Inc.) for 30 minutes at 37 °C and were then analyzed using a FACS Calibur. The activation of caspase-3 in cells was examined using the FACS Calibur after incubation with a fluoroscence isothiocyanate–labeled caspase-3 inhibitor peptide (FITC-DEVD-FMK, Calbiochem, San Diego, CA) for 1 hour at 37 °C.

Transduced K562 cells in a NOD/SCID xenograft model. Transduced K562 cells were affinity-purified by MACS using magnetic beads conjugated with an anti-human CD19 monoclonal antibody (Miltenyi Biotec Inc., Auburn, CA) or by FACS. The purity of the cells following isolation was evaluated using the FACS Calibur. NOD/SCID mice (5–8 weeks old, purchased from Jackson Laboratories, Bar Harbor, ME) were maintained at the Animal Resource Centre at the Princess Margaret Hospital (Toronto, ON, Canada). The entire animal experimental procedure followed a protocol approved by the Animal Care Committee of the University Health Network. Experimental groups consisted of male and female NOD/SCID mice injected with 2×10^7 K562 cells (re-suspended in 0.5 mL D-phosphate-buffered saline, Oxoid, Basingstoke, England) that were either lentivirally transduced ($n = 10$ animals for each LV construct) or NT ($n = 10$). Injections were performed subcutaneously into the dorsal right flanks of recipient mice as previously described.[49] One day after injection of the cells, half of the mice in each group ($n = 5$) began receiving daily AZT injections, administered intraperitoneally at a dose of 2.5 mg/kg/day for 14 days. Tumor growth was measured by caliper and calculated as $0.5 \times \text{length} \times \text{width}^2$ (in mm^3) for up to 14 days after inoculations.

Statistical analysis. Data are presented as the mean ± standard error of the mean for *in vitro* experiments and the mean ± standard deviation of the mean for *in vivo* experiments. Statistical analyses were performed using StatView version 4.5 software for Macintosh (SAS, Cary, NC). For *in vitro* experiments, a one-way analysis of variance with either a Bonferroni or a

Dunnett post hoc test was used to determine statistically significant results, with the level of significance set at $P < 0.05$. Statistical comparison of means was performed using a two-tailed unpaired Student's t-test for *in vivo* experiments.

ACKNOWLEDGMENTS

This work was supported by a National Cancer Institute of Canada/ Terry Fox Foundation Program Grant #014004 to J.A.M. We gratefully acknowledge Vanessa I. Rasaiah for helpful technical assistance.

REFERENCES

1. Hacein-Bey-Abina, S, Von Kalle, C, Schmidt, M, McCormack, MP, Wulffraat, N, Leboulch, P *et al.* (2003). LMO2-associated clonal T cell proliferation in two patients after gene therapy for SCID-X1. *Science* **302**: 415–419.
2. Roy, NS, Cleren, C, Singh, SK, Yang, L, Beal, MF and Goldman, SA (2006). Functional engraftment of human ES cell-derived dopaminergic neurons enriched by coculture with telomerase-immortalized midbrain astrocytes. *Nat Med* **12**: 1259–1268.
3. Nishiyama, Y and Rapp, F (1979). Anticellular effects of 9-(2-hydroxyethoxymethyl) guanine against herpes simplex virus-transformed cells. *J Gen Virol* **45**: 227–230.
4. Moolten, FL (1986). Tumor chemosensitivity conferred by inserted herpes thymidine kinase genes: paradigm for a prospective cancer control strategy. *Cancer Res* **46**: 5276–5281.
5. Mesnil, M and Yamasaki, H (2000). Bystander effect in herpes simplex virus-thymidine kinase/ganciclovir cancer gene therapy: role of gap-junctional intercellular communication. *Cancer Res* **60**: 3989–3999.
6. Kokoris, MS and Black, ME (2002). Characterization of herpes simplex virus type 1 thymidine kinase mutants engineered for improved ganciclovir or acyclovir activity. *Protein Sci* **11**: 2267–2272.
7. Qasim, W, Thrasher, AJ, Buddle, J, Kinnon, C, Black, ME and Gaspar, HB (2002). T cell transduction and suicide with an enhanced mutant thymidine kinase. *Gene Ther* **9**: 824–827.
8. Riddell, SR, Elliott, M, Lewinsohn, DA, Gilbert, MJ, Wilson, L, Manley, SA *et al.* (1996). T-cell mediated rejection of gene-modified HIV-specific cytotoxic T lymphocytes in HIV-infected patients. *Nat Med* **2**: 216–223.
9. Berger, C, Flowers, ME, Warren, EH and Riddell, SR (2006). Analysis of transgene-specific immune responses that limit the *in vivo* persistence of adoptively transferred HSV-TK-modified donor T cells after allogeneic hematopoietic cell transplantation. *Blood* **107**: 2294–2302.
10. Van Rompay, AR, Johansson, M and Karlsson, A (2000). Phosphorylation of nucleosides and nucleoside analogs by mammalian nucleoside monophosphate kinases. *Pharmacol Ther* **87**: 189–198.
11. Furman, PA, Fyfe, JA, St Clair, MH, Weinhold, K, Rideout, JL, Freeman, GA *et al.* (1986). Phosphorylation of 3'-azido-3'-deoxythymidine and selective interaction of the 5'-triphosphate with human immunodeficiency virus reverse transcriptase. *Proc Natl Acad Sci USA* **83**: 8333–8337.
12. St Clair, MH, Richards, CA, Spector, T, Weinhold, KJ, Miller, WH, Langlois, AJ *et al.* (1987). 3'-Azido-3'-deoxythymidine triphosphate as an inhibitor and substrate of purified human immunodeficiency virus reverse transcriptase. *Antimicrob Agents Chemother* **31**: 1972–1977.
13. Johnson, AA, Ray, AS, Hanes, J, Suo, Z, Colacino, JM, Anderson, KS *et al.* (2001). Toxicity of antiviral nucleoside analogs and the human mitochondrial DNA polymerase. *J Biol Chem* **276**: 40847–40857.
14. Lavie, A, Schlichting, I, Vetter, IR, Konrad, M, Reinstein, J and Goody, RS (1997). The bottleneck in AZT activation. *Nat Med* **3**: 922–924.
15. Brundiers, R, Lavie, A, Veit, T, Reinstein, J, Schlichting, I, Ostermann, N *et al.* (1999). Modifying human thymidylate kinase to potentiate azidothymidine activation. *J Biol Chem* **274**: 35289–35292.
16. Ostermann, N, Lavie, A, Padiyar, S, Brundiers, R, Veit, T, Reinstein, J *et al.* (2000). Potentiating AZT activation: structures of wild-type and mutant human thymidylate kinase suggest reasons for the mutants' improved kinetics with the HIV prodrug metabolite AZTMP. *J Mol Biol* **304**: 43–53.
17. Naldini, L, Blomer, U, Gallay, P, Ory, D, Mulligan, R, Gage, FH *et al.* (1996). *In vivo* gene delivery and stable transduction of nondividing cells by a lentiviral vector. *Science* **272**: 263–267.
18. Yoshimitsu, M, Sato, T, Tao, K, Walia, JS, Rasaiah, VI, Sleep, GT *et al.* (2004). Bioluminescent imaging of a marking transgene and correction of Fabry mice by neonatal injection of recombinant lentiviral vectors. *Proc Natl Acad Sci USA* **101**: 16909–16914.
19. Medin, JA and Karlsson, S (1997). Selection of retrovirally transduced cells to enhance the efficiency of gene therapy. *Proc Assoc Am Physicians* **109**: 111–119.
20. Sadelain, M and Riviere, I (2002). Sturm und drang over suicidal lymphocytes. *Mol Ther* **5**: 655–657.
21. Migita, M, Medin, JA, Pawliuk, R, Jacobson, S, Nagle, JW, Anderson, S *et al.* (1995). Selection of transduced CD34+ progenitors and enzymatic correction of cells from Gaucher patients, with bicistronic vectors. *Proc Natl Acad Sci USA* **92**: 12075–12079.
22. Medin, JA, Migita, M, Pawliuk, R, Jacobson, S, Amiri, M, Kluepfel-Stahl, S *et al.* (1996). A bicistronic therapeutic retroviral vector enables sorting of transduced CD34+ cells and corrects the enzyme deficiency in cells from Gaucher patients. *Blood* **87**: 1754–1762.
23. Qin, G, Takenaka, T, Telsch, K, Kelley, L, Howard, T, Levade, T *et al.* (2001). Preselective gene therapy for Fabry disease. *Proc Natl Acad Sci USA* **98**: 3428–3433.
24. Siatskas, C, Underwood, J, Ramezani, A, Hawley, RG and Medin, JA (2005). Specific pharmacological dimerization of KDR in lentivirally transduced human hematopoietic cells activates anti-apoptotic and proliferative mechanisms. *FASEB J* **19**: 1752–1754.
25. Medin, JA, Liang, SB, Hou, JW, Kelley, LS, Peace, DJ and Fowler, DH (2005). Efficient transfer of PSA and PSMA cDNAs into DCs generates antibody and T cell antitumor responses *in vivo*. *Cancer Gene Ther* **12**: 540–551.
26. Li, Z, Dullmann, J, Schiedlmeier, B, Schmidt, M, von Kalle, C, Meyer, J *et al.* (2002). Murine leukemia induced by retroviral gene marking. *Science* **296**: 497.
27. Doody, GM, Dempsey, PW and Fearon, DT (1996). Activation of B lymphocytes: integrating signals from CD19, CD22 and Fc gamma RIIb1. *Curr Opin Immunol* **8**: 378–382.
28. Fujimoto, M, Poe, JC, Hasegawa, M and Tedder, TF (2000). CD19 regulates intrinsic B lymphocyte signal transduction and activation through a novel mechanism of processive amplification. *Immunol Res* **22**: 281–298.
29. Tedder, TF, Zhou, LJ and Engel, P (1994). The CD19/CD21 signal transduction complex of B lymphocytes. *Immunol Today* **15**: 437–442.
30. Sato, S, Miller, AS, Howard, MC and Tedder, TF (1997). Regulation of B lymphocyte development and activation by the CD19/CD21/CD81/Leu 13 complex requires the cytoplasmic domain of CD19. *J Immunol* **159**: 3278–3287.
31. Greco, O and Dachs, GU (2001). Gene directed enzyme/prodrug therapy of cancer: historical appraisal and future prospectives. *J Cell Physiol* **187**: 22–36.
32. Mizuguchi, H, Xu, Z, Ishii-Watabe, A, Uchida, E and Hayakawa, T (2000). IRES-dependent second gene expression is significantly lower than cap-dependent first gene expression in a bicistronic vector. *Mol Ther* **1**: 376–382.
33. Coplan, NL and Bruno, MS (1989). Acquired immunodeficiency syndrome and heart disease: the present and the future. *Am Heart J* **117**: 1175–1177.
34. Sales, SD, Hoggard, PG, Sunderland, D, Khoo, S, Hart, CA and Back, DJ (2001). Zidovudine phosphorylation and mitochondrial toxicity *in vitro*. *Toxicol Appl Pharmacol* **177**: 54–58.
35. Masini, A, Scotti, C, Calligaro, A, Cazzalini, O, Stivala, LA, Bianchi, L *et al.* (1999). Zidovudine-induced experimental myopathy: dual mechanism of mitochondrial damage. *J Neurol Sci* **166**: 131–140.
36. Smiley, ST, Reers, M, Mottola-Hartshorn, C, Lin, M, Chen, A, Smith, TW *et al.* (1991). Intracellular heterogeneity in mitochondrial membrane potentials revealed by a J-aggregate-forming lipophilic cation JC-1. *Proc Natl Acad Sci USA* **88**: 3671–3675.
37. Green, DR and Reed, JC (1998). Mitochondria and apoptosis. *Science* **281**: 1309–1312.
38. Omar, RF, Gourde, P, Desormeaux, A, Tremblay, M, Beauchamp, D and Bergeron, MG (1996). *In vivo* toxicity of foscarnet and zidovudine given alone or in combination. *Toxicol Appl Pharmacol* **139**: 324–332.
39. Cazzalini, O, Lazze, MC, Iamele, L, Stivala, LA, Bianchi, L, Vaghi, P *et al.* (2001). Early effects of AZT on mitochondrial functions in the absence of mitochondrial DNA depletion in rat myotubes. *Biochem Pharmacol* **62**: 893–902.
40. McKee, EE, Bentley, AT, Hatch, M, Gingerich, J and Susan-Resiga, D (2004). Phosphorylation of thymidine and AZT in heart mitochondria: elucidation of a novel mechanism of AZT cardiotoxicity. *Cardiovasc Toxicol* **4**: 155–167.
41. Mahmoud, MS, Fujii, R, Ishikawa, H and Kawano, MM (1999). Enforced CD19 expression leads to growth inhibition and reduced tumorigenicity. *Blood* **94**: 3551–3558.
42. Bonini, C, Ferrari, G, Verzeletti, S, Servida, P, Zappone, E, Ruggieri, L *et al.* (1997). HSV-TK gene transfer into donor lymphocytes for control of allogeneic graft-versus-leukemia. *Science* **276**: 1719–1724.
43. Cohen, JL, Boyer, O, Salomon, B, Onclercq, R, Charlotte, F, Bruel, S *et al.* (1997). Prevention of graft-versus-host disease in mice using a suicide gene expressed in T lymphocytes. *Blood* **89**: 4636–4645.
44. Spencer, DM (2000). Developments in suicide genes for preclinical and clinical applications. *Curr Opin Mol Ther* **2**: 433–440.
45. Lal, S, Lauer, UM, Niethammer, D, Beck, JF and Schlegel, PG (2000). Suicide genes: past, present and future perspectives. *Immunol Today* **21**: 48–54.
46. Kershaw, MH, Teng, MW, Smyth, MJ and Darcy, PK (2005). Supernatural T cells: genetic modification of T cells for cancer therapy. *Nat Rev Immunol* **5**: 928–940.
47. Chow, HH, Li, P, Brookshier, G and Tang, Y (1997). *In vivo* tissue disposition of 3'-azido-3'-deoxythymidine and its anabolites in control and retrovirus-infected mice. *Drug Metab Dispos* **25**: 412–422.
48. Jung, U, Foley, JE, Erdmann, AA, Eckhaus, MA and Fowler, DH (2003). CD3/CD28-costimulated T1 and T2 subsets: differential *in vivo* allosensitization generates distinct GVT and GVHD effects. *Blood* **102**: 3439–3446.
49. Weichold, FF, Jiang, YZ, Dunn, DE, Bloom, M, Malkovska, V, Hensel, NF *et al.* (1997). Regulation of a graft-versus-leukemia effect by major histocompatibility complex class II molecules on leukemia cells: HLA-DR1 expression renders K562 cell tumors resistant to adoptively transferred lymphocytes in severe combined immunodeficiency mice/nonobese diabetic mice. *Blood* **90**: 4553–4558.

Original Paper

Pharmacology

Pharmacology 2008;81:251–258
DOI: 10.1159/000114719

Received: February 23, 2007
Accepted: October 10, 2007
Published online: February 4, 2008

Potentiation of Potassium Currents by Beta-Adrenoceptor Agonists in Human Urinary Bladder Smooth Muscle Cells: A Possible Electrical Mechanism of Relaxation

Jun Takemoto[a–c] Haruko Masumiya[a] Kazuo Nunoki[d] Takeya Sato[a, c]
Haruo Nakagawa[b] Yoshihiro Ikeda[b] Yoichi Arai[b] Teruyuki Yanagisawa[a, c]

Departments of [a]Molecular Pharmacology and [b]Urology, Graduate School of Medicine, Tohoku University, and [c]Tohoku University 21st Century COE Program 'Comprehensive Research and Education Center for Planning of Drug and Clinical Evaluation, CRESCENDO', Sendai, and [d]Department of Human Health and Nutrition, Shokei Gakuin University, Natori, Japan

Key Words
Ca^{2+}-activated K^+ (K_{Ca}) channels · Iberiotoxin · Apamin · BRL 37344 · Patch clamp, whole-cell

Abstract
We examined the effects of β-adrenoceptor agonists on the membrane currents of smooth muscle cells from the human urinary bladder using a whole-cell patch clamp to investigate the involvement of Ca^{2+}-activated K^+ (K_{Ca}) channels in relaxation by β-adrenergic agonists. With 0.05 mmol/l EGTA in the patch pipette, depolarizing pulses evoked outward rectifying currents. Isoproterenol (1 μmol/l) significantly increased the membrane currents by 75% at +80 mV with 0.05 mmol/l EGTA pipette solution. BRL 37344 (1 μmol/l) significantly increased the membrane currents by 44% at +80 mV. Iberiotoxin (100 nmol/l) significantly decreased the membrane currents by 60% at +80 mV. In the presence of iberiotoxin, the potentiation of the outward currents by isoproterenol was greatly suppressed and, in the presence of iberiotoxin and apamin (1 μmol/l), the potentiation by isoproterenol was totally abolished. On the other hand, with 5 mmol/l EGTA pipette solution, depolarizing pulses evoked smaller outward currents. Isoproterenol (1 μmol/l) did not change the membrane currents with 5 mmol/l EGTA pipette solution. The real-time PCR analysis revealed the expression of β_2-adrenoceptors in the cells. These results suggest that Ca^{2+}-activated and iberiotoxin- and apamin-sensitive currents via both large-conductance and small-conductance K_{Ca} channels could be increased by stimulation of β_2-adrenoceptors.

Introduction

It has been shown that β-adrenoceptor agonists exert potent relaxant effects on the detrusor muscle of the bladder in various species [1–3] and β-adrenoceptors of the detrusor muscle are a potential therapeutic target for overactive bladder. The effects of β-adrenoceptor agonists on smooth muscle are generally considered to be mediated by intracellular cyclic adenosine monophosphate (cAMP) through stimulation of adenylyl cyclase via stimulatory G protein coupled to the β-adrenoceptors (briefly reviewed by Tanaka et al. [4]) and it has also been suggested that relaxation of the smooth muscles by β-adrenoceptor agonists results from phosphorylation by cAMP-dependent protein kinase (PKA) of the contractile machinery of smooth muscle including myosin light-

KARGER
Fax +41 61 306 12 34
E-Mail karger@karger.ch
www.karger.com

0031–7012/08/0813–0251$24.50/0

Accessible online at:
www.karger.com/pha

Teruyuki Yanagisawa
2-1 Seiryo-machi
Aoba-ku
Sendai, 980-8575 (Japan)
Tel. +81 22 717 8061, Fax +81 22 717 8065, E-Mail yanagswt@mail.tains.tohoku.ac.jp

chain kinase [5], although some discrepancies exist between the increases in cAMP and the relaxation of canine coronary arterial smooth muscle [6], and between the inhibition of adenylyl cyclase or PKA and that of relaxation of rat urinary bladder [7]. Various recent studies have examined the effects of β-adrenoceptor agonists on the excitability of the membrane and contractility of smooth muscle. It has been shown that the hyperpolarization induced by the opening of various type K^+ channels in smooth muscles results in relaxation, that is 'hyperpolarization-relaxation coupling' [8]. In detrusor smooth muscle cells of guinea pigs, it was suggested that isoproterenol probably hyperpolarized the membrane by stimulating the sodium pump activity and preventing spontaneous action potentials [9]. Kobayashi et al. [10] showed that the relaxation of guinea pig bladder smooth muscle by isoproterenol had a causal relation to the increase in large-conductance Ca^{2+}-activated K^+ (BK_{Ca}) currents subsequent to activation of the cAMP/PKA pathway. It was also shown in guinea pig urinary bladder smooth muscle that BK_{Ca} channels are activated indirectly by β-adrenoceptor agonists through Ca^{2+} influx through voltage-dependent L-type Ca^{2+} channels and Ca^{2+} sparks [11]. However, the effects of β-adrenoceptor stimulation on the membrane currents of smooth muscle cells of human urinary bladder have not been reported.

The β-adrenoceptors of human detrusor muscle were shown not to have functional characteristics typical of β_1- or β_2-adrenoceptors [12]. Based on the rank order of the potency of agonists, in vitro relaxation studies have demonstrated that the β_3-adrenoceptor is predominantly involved in the relaxation of human detrusor muscle [13, 14]. With the use of quantitative reverse-transcription polymerase chain reaction (RT-PCR), it has also been demonstrated that human detrusor muscles from normal and obstructed bladders predominantly express β_3-adrenoceptor messenger RNA (mRNA), although those of β_1- and β_2-receptors are expressed at lower levels [15]. Taken together, it seems likely that the subtype of β-adrenoceptors involved in relaxation is predominantly β_3 in human detrusor muscle.

In the present study we examined the effects of isoproterenol and BRL 37344, a β_3-adrenoceptor agonist with β_2-adrenoceptor affinity [16, 17], on the membrane currents of smooth muscle cells from human urinary bladder to investigate the possibility that hyperpolarization by an increase in outward Ca^{2+}-activated K^+ (K_{Ca}) current might be involved in the relaxation of the human urinary bladder by β-adrenoceptor stimulation.

Materials and Methods

Cell Culture

Smooth muscle cells of human urinary bladder were obtained from Cambrex Bio Science (Walkersville, Md., USA). The smooth muscle cells were cultured in SmGM-2 medium (Cambrex) containing 5% fetal bovine serum, gentamicin (50 mg/l) and amphotericin B (50 μg/l) at 37°C under 5% CO_2. Smooth muscle cells of human urinary bladder between passages 6 and 8 were used for the experiments.

Electrophysiological Recordings

Membrane currents were recorded with a whole-cell voltage clamp method using an amphotericin B perforated patch (90 μg/ml). Pipettes with a resistance ranging from 5 to 9 MΩ were filled with pipette solution of the following composition (in mmol/l): 110 potassium aspartate, 30 KCl, 10 NaCl, 1 $MgCl_2$, 10 HEPES, and either 0.05 or 5 EGTA (pH 7.30 with KOH). The external solution was of the following composition (in mmol/l): 135 NaCl, 5.4 KCl, 1.8 $CaCl_2$, 1 $MgCl_2$, 5 HEPES, 11.1 glucose (pH 7.35 with NaOH). The liquid junction potential between the pipette and external solution was corrected before the seal formation [18–20]. After the formation of a gigaohm seal, the pipette capacitance was compensated before the membrane currents were recorded. Series resistance was compensated, and currents were filtered at 1 kHz and recorded at a sampling frequency of 5 kHz. Data acquisition and analysis were performed with a patch clamp amplifier (Axopatch 200B, Axon Instruments, Foster City, Calif., USA), a personal computer and pCLAMP software (version 8.0.2, Axon instruments). All experiments were performed at room temperature (23–25°C).

RNA Extraction and Complementary DNA Synthesis and Real Time RT-PCR Analysis

mRNA was purified from the primary cultured human urinary bladder smooth muscle cells using oligo-dT magnetic beads (Miltelnyi Biotec, Bergisch Gladbach, Germany) according to the manufacturer's protocol. Complementary DNA (cDNA) generated from mRNA used as templates was synthesized by reverse transcription using an oligo-dT primer and Primescript™ reverse transcriptase (Takara Bio, Tokyo, Japan).

Real-time PCR was performed using a 7500 real-time PCR system (Applied Biosystems, Foster City, Calif., USA) with the specific forward and reverse primers and the hybridization probe DNA for each of the human β-adrenoceptor subtypes and human glyceraldehyde-3-phosphate dehydrogenase (GAPDH) mRNAs to determine the copy numbers of the target cDNA in each sample. The reaction conditions used were as follows: 50°C, 2 min, then 94°C, 2 min, and then 45 cycles of 94°C, 30 s, and 60°C, 1 min. Data for the amplification of the target sequence were collected during the 60°C step. The plasmid DNA carrying either the cDNA for each subtype of human β-adrenoceptors [17] or human GAPDH was used as a standard for each assay. Relative quantitation results were measured using the comparative cycle threshold method, whereby the amplification of the gene of interest is normalized to that of the gene encoding GAPDH measured from the same cDNA sample. The sequences of the forward and the reverse primers and the hybridization probes were as follows: 5′-GACGACGACGACGATGT-3′, 5′-CTTGGATTCCGAGGCGAAGC-TAMRA-3′ and 5′-F-FAM-CGGCACGGCTCGTCCAG-

GCTCG-TAMRA-3′ for human β_1-adrenoceptor; 5′-CCTTCT-TGCTGGCACCCAAT-3′, 5′-CCAGGACGATGAGAGACATG-AC-3′ and 5′-FAM-ATGCCCACCACCCACACCTCGTC-TAM-RA-3′ for human β_2-adrenoceptor; 5′-CGTTACGGCGCAC-TGGTCAC-3′, 5′-TGGCTCATGATGGGCGCAAAC-3′ and 5′-F-FAM-CGGCACGGCTCGTCCAGGCTCG-TAMRA-3′ for human β_3-adrenoceptor; 5′-CCAAGGTCATCCATGACAACTT-TG-3′, 5′-CGGCCATCACGCCACAG-3′ and 5′-FAM-AGTCC-ATGCCATCACTGCCACCCAG-TAMRA-3′ for human GAPDH, respectively.

Drugs

Amphotericin B, isoproterenol, iberiotoxin and apamin were purchased from Sigma (St. Louis, Mo., USA). BRL 37344 [(R*,R*)-(±)-4-(2-[(2-[3-chlorophenyl]-2-hydroxyethyl)amino]propyl)-phenoxyacetic acid] was purchased from Tocris (Ellisville, Mo., USA). All other chemicals were of the highest grade commercially available. The drugs were added to the bath solution from a stock solution (<1 mmol/l) in distilled water. Amphotericin B was dissolved in 100% dimethyl sulfoxide. The final concentration of dimethyl sulfoxide (0.15%) did not affect the measured electrophysiological parameters.

Statistics

All experimental data are presented as means ± SEM. The statistical significance of difference between the means was evaluated by 1-way analysis of variance followed by either paired or unpaired t tests; p values less than 0.05 were considered significant.

Results

Effects of Isoproterenol and BRL 37344 on the Membrane Currents of Smooth Muscle Cells from Human Urinary Bladder

The membrane currents of smooth muscle cells from human urinary bladder were elicited by test pulses from a holding potential of −80 mV to voltages between −100 mV and +80 mV. Figure 1A shows representative traces of the membrane currents recorded with pipette solution containing 0.05 mmol/l EGTA. Outward membrane currents were activated at −20 mV and were gradually increased with further depolarization until +80 mV. The outward currents with prominent fluctuation were maintained during depolarization without distinct inactivation and time-dependent activation.

The effects of isoproterenol on the currents of smooth muscle from human urinary bladder with 0.05 mmol/l EGTA pipette solution were examined. Figure 1A shows the representative traces of membrane currents recorded in the absence and presence of 1 μmol/l isoproterenol. Isoproterenol increased both inward and outward currents. The current-voltage (I–V) relationships of the membrane currents were obtained by plotting the maximal inward or outward current density during a test pulse versus the membrane potential. The I–V curves show that isoproterenol increased the maximal membrane current densities at test potentials more positive than −20 mV (fig. 1B). Isoproterenol significantly increased the maximal membrane current densities from 7.18 ± 1.27 to 12.51 ± 2.66 pA/pF at +80 mV (n = 5, p = 0.037). With 0.05 mmol/l EGTA pipette solution, isoproterenol (0.01–1 μmol/l) increased the maximal membrane current densities at +80 mV in a concentration-dependent manner (fig. 1C). The increase with 10 μmol/l isoproterenol tended to be smaller than that with 1 μmol/l (data not shown).

It has been suggested that the β_3-adrenoceptor is predominantly involved in the relaxation of human detrusor muscle. We examined whether BRL 37344, a β_2- and β_3-adrenoceptor partial agonist, increases the membrane currents of smooth muscle cells of human urinary bladder. With 0.05 mmol/l EGTA pipette solution, 1 μmol/l BRL 37344 increased both inward and outward currents, especially the membrane current densities at voltages more positive than +20 mV (fig. 1D). BRL 37344 (1 or 10 μmol/l) increased the maximal membrane current densities from 4.06 ± 0.86 to 6.41 ± 1.50 pA/pF (n = 6, p = 0.043) or from 6.00 ± 2.27 to 8.59 ± 3.02 pA/pF (n = 5, p = 0.060), respectively at +60 mV, and from 7.09 ± 0.83 to 10.51 ± 1.95 pA/pF (n = 6, p = 0.032) or from 9.28 ± 2.79 to 13.13 ± 3.98 pA/pF (n = 5, p = 0.039), respectively at +80 mV. The percentage increases at +80 mV produced by BRL 37344 in 2 concentrations were almost the same, that is 44 ± 10% (n = 6, 1 μmol/l) and 44 ± 7% (n = 5, 10 μmol/l), respectively (fig. 1C) The BRL-37344-induced increase in the membrane currents was 59% of that of 1 μmol/l isoproterenol (+75 ± 22%, n = 5).

These results indicate that both isoproterenol and BRL 37344 increased the membrane currents of the smooth muscle cells, but, the efficacy of BRL 37344 was about one half of that of isoproterenol.

Effects of Iberiotoxin and Apamin on the Membrane Currents

We examined the effects of iberiotoxin, a BK_{Ca} channel blocker, on the membrane currents in the smooth muscle cells and on the potentiation of the outward currents by isoproterenol with 0.05 mmol/l EGTA pipette solution. Figure 2A shows the representative traces of membrane currents in the absence and presence of 100 nmol/l iberiotoxin and with the subsequent addition of 1 μmol/l isoproterenol. The I–V curves show that iberiotoxin significantly decreased the maximal outward membrane current densities, and subsequent addition of iso-

proterenol significantly increased the attenuated currents at test potentials of +60 mV and +80 mV. The maximal membrane current densities at +80 mV in the absence and the presence of iberiotoxin, and presence of both iberiotoxin and isoproterenol were 10.22 ± 1.85, 3.86 ± 0.65, and 5.31 ± 0.77 pA/pF (n = 6), respectively. The increase in current was much smaller than the control isoproterenol response. We examined the effects of apamin, a small-conductance Ca^{2+}-activated K^+ (SK_{Ca}) channel blocker, on the membrane currents and on the potentiation of the outward currents by isoproterenol with 0.05 mmol/l EGTA pipette solution. The maximal membrane current densities at +80 mV in the absence and presence of apamin, and the presence of both apamin and isoproterenol were 13.20 ± 2.30, 10.74 ± 2.01, and 16.77 ± 3.07 pA/pF, respectively (n = 5). Although apamin tended to decrease the outward current, the potentiation by isoproterenol could not be greatly inhibited by

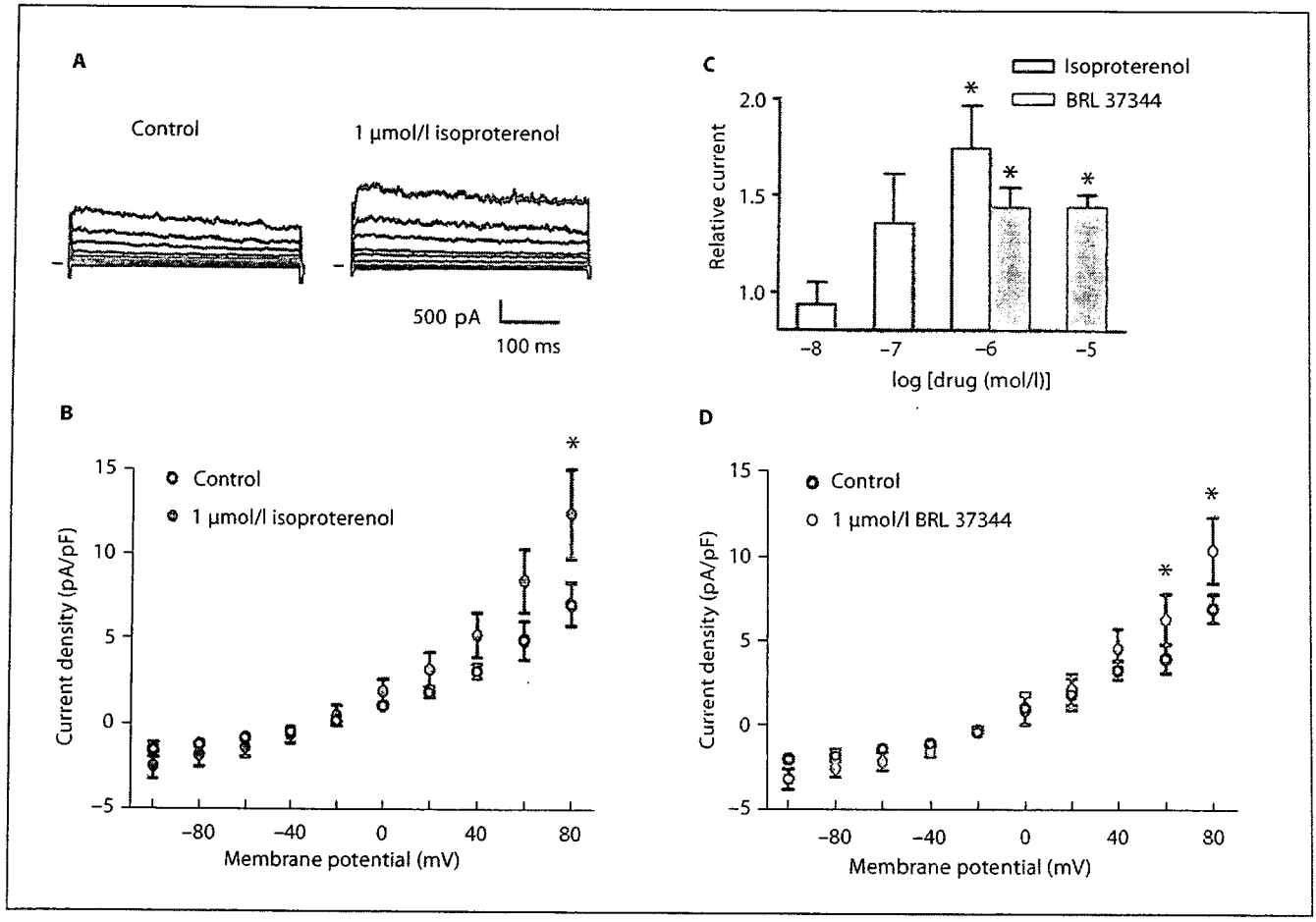

Fig. 1. Isoproterenol and BRL 37344 increased the membrane currents of smooth muscle cells from human urinary bladder. **A** Representative current traces before (left) and during (right) application of 1 μmol/l isoproterenol with low EGTA (0.05 mmol/l) pipette solution. Membrane currents were elicited by 400-ms test pulses from a holding potential of −80 mV to potentials from −100 to +80 in 20-mV steps. Horizontal bars before the current traces indicate zero current level. **B** Current-voltage relationships of membrane currents in the absence (○) and presence (●) of 1 μmol/l isoproterenol. Values indicate means ± SEM of 5 experiments. * p = 0.037 versus control. **C** Concentration-response relationships of isoproterenol and BRL 37344. Membrane currents were elicited by a 400-ms depolarizing test pulse to +80 mV from a holding potential of −80 mV in the absence and presence of each isoproterenol (n = 5) and BRL 37344 concentration. Relative currents versus control were calculated. * $p < 0.05$ versus control (1 μmol/l isoproterenol, n = 5, p = 0.037; 1 μmol/l BRL 37344, n = 6, p = 0.032; 10 μmol/l BRL 37344, n = 5, p = 0.039). **D** Current-voltage relationships of membrane currents in the absence (○) and presence (●) of 1 μmol/l BRL 37344 (n = 6). * $p < 0.05$ versus control (p = 0.043 at +60 mV; p = 0.032 at +80 mV).